International Journal of Industrial Chemistry (IJIC)
a SpringerOpen Journal

RESEARCH Open Access

Modeling of fluidized bed reactor for ethylene polymerization: effect of parameters on the single-pass ethylene conversion

Hassan Farag[1], Mona Ossman[2,3], Moustapha Mansour[1] and Yousra Farid[1*]

Abstract

Background: In this study, we present the developments in modeling gas-phase catalyzed olefin polymerization fluidized bed reactors (FBR) using chromium catalyst technique. The model is based on the two-phase theory of gas-solid fluidization: bubble phase and emulsion phase. The model has proved to be the suitable model in many of past studies. In the proposed model, the bed is divided into several sequential sections. The effect of important reactor parameters such as superficial gas velocity, catalyst injection rate, catalyst particle growth, and minimum fluidization velocity on the dynamic behavior of the FBR has been discussed. The conversion of product in a fluidized bed reactor is investigated and compared with the actual data from the plant site.

Results: A good agreement has been observed between the model predictions and the actual plant data. It has been shown that about 0.28% difference between the calculated and actual conversions has been achieved.

Conclusions: The study showed that the computational model was capable of predicting the hydrodynamic behavior of gas-solid fluidized bed flows with reasonable accuracy.

Keywords: Fluidized bed reactor, Mathematical model, Ethylene conversion, Bed height, Catalyst feed rate

Background

The fluidized bed reactor has a unique physical design, with gas and polymer particles flowing in opposite directions. It consists of metallic catalyst particles that are fluidized by the flow of ethylene gas, and catalyst particles (pre-polymer) are suspended in the ethylene fluid as ethylene gas is pumped from the bottom of the reactor bed to the top. The gas is fed from the base of the reactor and splits into two phases: bubble phase and emulsion phase. Pre-polymer particles are fed in near the top of the reactor, and while the polymerization reaction occurs, the particles grow, increasing in weight and size. Particle segregation occurs in the reactor according to particle weight, so the full-grown polymer particles are removed at the base of the reactor. Non-reacted gases leave the reactor after passing through the disengagement zone [1]. Pre-polymerization is generally carried out in continuous stirred-tank reactors (CSTR) located before the fluidized bed reactor. Catalyst particles are fed into the CSTR along with ethylene and co-monomers to yield pre-polymer. Afterwards, these pre-polymerized catalyst particles are fed into the FBR to complete the ethylene polymerization. A diagram of the industrial fluidized bed reactor system using a CSTR as the pre-polymerization reactor is shown in Figure 1 [2]. In effect, the catalyst is not actually consumed; it is simply incorporated with the polyethylene product as polyethylene molecules remain stuck to the catalyst particle from which they were produced.

The conversion of ethylene is low for a single pass through the reactor, and it is necessary to recycle the unreacted ethylene. Unreacted ethylene gas is removed off the top of the reactor, where it is expanded and decompressed to separate the catalyst and low molecular weight polymer from the gas. After purification, ethylene gas is then recompressed and recycled back into the reactor. Granular polyethylene is gradually removed from the bottom of the reactor as soon as reasonable conversions have been achieved. Typically, a residence time of 3 to 5 h results in a 97% conversion of ethylene.

* Correspondence: Eng_yousra_hamdy@yahoo.com
[1]Chemical Engineering Department, Faculty of Engineering, Alexandria University, Alexandria, Egypt
Full list of author information is available at the end of the article

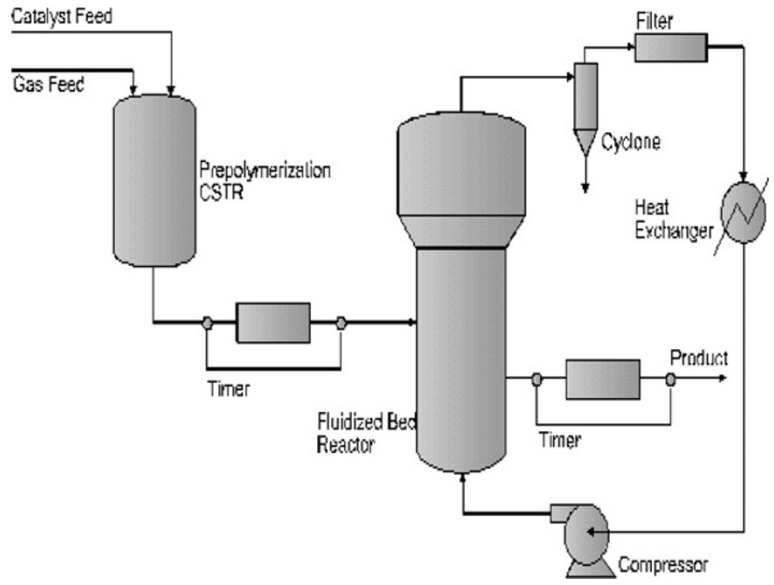

Figure 1 Industrial polyethylene production diagram (BP Chemical Technology, London).

The flow in the fluidized bed reactor can be mathematically modeled using mole balances [1].

An accurate model describing the movement of gas/solid and pressure distribution around a rising bubble was then proposed by Davidson and Harrison [3].This model describes the gas flow through a three dimensional fluidized bed mainly in spherical or semi-spherical shape bubbles through the core; however, depending on the emulsion gas velocity, the region around the bubble may be surrounded by a cloud as a result of emulsion gas circulation between the dense solid phase and the core of the bubble.

Choi and Ray [4] proposed a two-phase model including bubble and emulsion phases with constant bubble size. McAuley et al. [5] proposed a single phase model by modifying Ray's model with additional assumptions. In a comparison between the two models, they have shown that the single phase assumption does not make considerable difference in the results obtained from the models. Hatzantonis et al. [6] in a research work developed the two-phase model by considering the bubble growth effect on hydrodynamic behavior of the reactor and have shown that the developed model has a better agreement with industrial data than single-phase and two-phase models with constant bubble size. Grosso and Chiovetta [7] studied the particle size distribution in the output stream of commercial, fluidized bed reactors for ethylene polymerization using the mathematical model. In another work, Kiashemshaki et al. [8] developed the two-phase model by considering the polymerization reaction not only in the emulsion phase but also in the bubble phase. They have indicated that about 20% of the polymerization reaction occurs in the bubble phase.

Vahidi and Shahrokhi [9] studied the dynamic behavior and control of a fluidized bed reactor for polyethylene production. It has been shown that the control system has satisfactory performances either for set point tracking or load rejection. Hamzehei [10] studied the heat transfer of a poly ethylene fluidized bed reactor without reaction experimentally and computationally at different superficial gas velocities.

The advantage of the present work over the previous ones is that it considered major factors that affect the fluidized bed reactor model, like the bubble size, particle size distribution, and catalyst properties in dynamic simulation of the reactor in order to obtain better understanding of the reactor performance. In the present study, a FBR model is developed to be able to predict the main factors affecting the ethylene conversion. Simulation results indicate that this strategy promotes the control performance considerably.

Methods

Model assumptions

The model assumes the following:

1 The reactor operates at a steady state, under uniform temperature.
2 The reactor is in isothermal operation.
3 The gas flows in plug flow, with gas interchange between phases.

Table 1 Operating conditions and simulation (Sidpec Petrochemical Company)

Parameter	Unit	Value/type
Monomer properties		
Ethylene feed concentration	mol m^{-3}	4×10^{-4}
Hydrogen feed concentration	mol m^{-3}	9.6×10^{-5}
Actual ethylene conversion per pass	%	3.33
Overall ethylene conversion	%	100
Catalyst properties		
Type of catalyst		Silica base chromium catalyst with Al and Ti modifiers
Cr consumption	ppm	5 ppm/1 ton residual polymer
Prepolymer properties		
Prepolymer density	Kg m^{-3}	2,380
Prepolymer particle size	m	190×10^{-6}
Prepolymer feed rate	Kg s^{-1}	0.013
Polymer properties		
Polymer density	Kg m^{-3}	955
Polymer average particle size	m	1.166×10^{-3}
Flow rate of polymer product	Kg s^{-1}	4.16
Minimum particle size	m	1.070×10^{-3}
Maximum particle size	m	1.215×10^{-3}
Density function(PSD)	1/m	0.6489
Particle size distribution	1/m	Range from 190 to 1,215 μ
Reactor parameter		
Temperature	°C	108
Pressure	bar	21.5
Diameter	m	5
Fluidizing velocity	M s^{-1}	0.56
Bed height	m	16
Maximum reactor height	m	22
Bed voidage ε_{mf}	-	0.5
Inert gas properties		
Gas density	Kg m^{-3}	17.05
Composition (% volume)		13.02
Ethylene		14.7
Hydrogen		47.2
Nitrogen		19.06
Ethane		6
Butane		1.08×10^{-2}
Butene-1		

4 The bed is axially divided into N compartments, each one consisting of the bubble, cloud, and emulsion phases.
5 Bubbles grow continuously along the reactor height from their initial diameter until they reach the maximum stable bubble diameter.
6 The bed volume fraction occupied by bubbles and emulsion depends on the flow regime and changes along the reactor height.
7 Solid entrainment and carryover are taken into account by the model. However, particle agglomeration and breakage are not considered.

8 Bed voidage is constant from the distributor until H_{mf} and is equal to 0.5.

Model development

Minimum fluidizing velocity

The superficial gas velocity at minimum fluidization conditions is calculated from the correlations gives by Kunii and Levenspiel [11]:

$$U_{mf} = \frac{Re_{mf}\mu_g}{\rho_g d_p} \tag{1}$$

$$Ar = \frac{g d_p^3 \rho_g \left(\rho_p - \rho_g\right)}{\mu_g^2} \tag{1a}$$

$$Re_{mf} = \left[(33.7)^2 + 0.0408Ar\right]^{0.5} - 33.7, \tag{1b}$$

where viscosity of the gas mixture is given by the following relation [12]:

$$\mu_{g,\mathrm{mix}=} \frac{\sum y_j \mu_j M_j^{1/2}}{\sum y_j M_j^{1/2}}. \tag{1c}$$

Bubble growth equations

Bubble growth diameter at corresponding bed height is calculated by the correlation given by Wen and Fan [13].

$$\mathrm{b_{di}} = 0.14\mathrm{d_p}\rho_\mathrm{p}\left(\frac{\mathrm{U}_g}{\mathrm{U_{mf}}}\right)\mathrm{h_i} + \mathrm{d_{bo}}. \tag{2}$$

Initial bubble diameter forms near the distributor calculated from the correlations given by Kunii and Levenspiel [11]:

$$d_{\mathrm{bo}} = \frac{2.78\left(U_g - U_{\mathrm{mf}}\right)^2}{g}. \tag{2a}$$

The Mori and Wen [14] relation is used to obtain the maximum bubble diameter:

$$d_{\mathrm{bm}} = 0.65\left(S\left(U_g - U_{\mathrm{mf}}\right)\right)^{0.4}\mathrm{cm}. \tag{2b}$$

Kunii and Levenspiel [11] correlation is used to calculate the bubble rising velocity:

$$U_{bi} = U_g - U_{\mathrm{mf}} + 0.711\left(\mathrm{gd}_{bi}\right)^{1/2}. \tag{2c}$$

The relative fraction of the bubble phase for the ith compartment is given by Kunii and Levenspiel [11]:

$$\delta_i = \frac{\left(U_g - U_{\mathrm{mf}}\right)}{\left(U_{bi} - U_{\mathrm{mf}}\right)}. \tag{2d}$$

The average bubble fraction calculated from the correlations given by Cui et al. (2000) [15]:

$$\delta = 0.534\left[\frac{1 - \exp\left(U_g - U_{\mathrm{mf}}\right)}{0.413}\right]. \tag{2e}$$

Kobayashi et al. [16] correlation is used to calculate the number of bubbles:

$$N_i = \frac{6S(H - H_{\mathrm{mf}})}{\pi H \Delta h_i^2}, \tag{2f}$$

where the U_{br} is given by the correlation of Grace [17]:

$$U_{\mathrm{br},i} = 0.711(g d_{bi})^{1/2}. \tag{2g}$$

Compartment height

Consider the following equations for the compartment height:

$$\Delta h_i = 2d_{\mathrm{bo}}\frac{(2+m)^{i-1}}{(2-m)^i} \tag{3}$$

$$\Delta h_1 = d_{\mathrm{bo}} + \left(1 - \frac{m}{2}\right), \tag{3a}$$

where

$$m = 1.4 d_p \rho_p \frac{U_g}{U_{\mathrm{mf}}}. \tag{3b}$$

The total compartment height is calculated using the following equation:

$$H_n = \sum_{i=1}^{n} \Delta h_i \tag{3c}$$

Height at minimum fluidizing conditions

Height at minimum fluidizing conditions is calculated by the correlation given by McAuley et al. [5].

$$H_{\mathrm{mf}} = H(1 - \delta). \tag{4}$$

Maximum bubble diameter

Haider and Levenspiel [18] correlation is used to calculate the terminal falling velocity:

$$d_{b,max} = \frac{2U_t^2}{g} \tag{5}$$

$$d_p^{'} = 2.7 d_p \tag{5a}$$

$$d_p^{*} = d_p^{'}\left[\mu_g^{-2}\rho_g\left(\rho_p - \rho_g\right)g\right]^{1/3} \tag{5b}$$

$$U_t^{*} = \left[18 d_p^{*-2} + (2.335 - 1.744\Phi_s) d_p^{*-\frac{1}{2}}\right]^{-1} \tag{5c}$$

$$U_t = U_t^{*}\left[\mu_g\rho_g^{-2}\left(\rho_p - \rho_g\right)g\right]^{\frac{1}{3}}. \tag{5d}$$

Diffusion of ethylene

Specchia et al. [19] correlation is used to calculate the self diffusion of ethylene:

$$D_A = s\frac{U_g d_p}{8.65\left(1 + 1.94\left(\frac{d_p}{D}\right)^2\right)}. \tag{6}$$

Mass transfer coefficient

Mass transfer coefficient is calculated by the correlation gives by Kunii and Levenspiel [20].

$$K_{\mathrm{be},i} = \left[\left(\frac{1}{K_{\mathrm{bc},i}}\right) + \left(\frac{1}{K_{\mathrm{ce},i}}\right)\right]^{-1} \tag{7}$$

$$K_{b,i} = 4.5\frac{U_{\mathrm{mf}}}{d_{b,i}} + \frac{5.85\left(D_A^{1/2} g^{1/4}\right)}{d_{bi}^{\frac{5}{4}}} \tag{7a}$$

$$K_{e,i} = 6.78\left(\frac{\varepsilon_{\mathrm{mf}} D_A U_{b,i}}{d_{bi}^3}\right)^{1/2} \tag{7b}$$

Bed voidage

Bed voidage is calculated by the correlation given by Wen and Fan [13]:

$$(1 - \varepsilon) = \frac{H_{mf}\left(1 - \varepsilon_{mf}\right)}{H} \tag{8}$$

for $h \le H_{\mathrm{mf}}$

$$(1 - \varepsilon_i) = \frac{H_{\mathrm{mf}}}{H(1 - \varepsilon_{\mathrm{mf}})} - \frac{H_{\mathrm{mf}}(1 - \varepsilon_{\mathrm{mf}})(h - H_{\mathrm{mf}})}{2H(H - H_{\mathrm{mf}})} \tag{8a}$$

for $H_{\mathrm{mf}} \le h \le [H_{\mathrm{mf}} + 2(H - H_{\mathrm{mf}})]$.

Particle size distribution of polymer

Grosso and Chiovetta [7] give a correlation to calculate the particle size distribution of the polymer and for the catalyst feed particles:

$$P_b(d_p) = \frac{\left(3\, d_p^5\, \rho_p{}^2 \chi_{\mathrm{cat}}^2\right)}{d_{\mathrm{po}}^6 \rho_{\mathrm{cat}}^2 (1 - \chi_{\mathrm{cat}})} * \frac{\left\{1 + \left(\frac{d_p^3}{d_{\mathrm{po}}^3}\right)\left[\left(\frac{\rho_{\mathrm{cat}}}{\rho_{\mathrm{cat}}} - 1\right)\right]\right\}\exp\left[\rho_p \chi_{\mathrm{cat}}\left(d_{p^2} - dp_o^3\right)\right]}{\rho_{\mathrm{cat}} dp^3 (1 - \chi_{\mathrm{cat}})} \tag{9}$$

$$P_o(r) = \int_{d_{\mathrm{po}}}^{d_p} P_b(d_p) d_p\, d(d_p) \left\{\int_{d_{\mathrm{po}}}^{dp}\left[P_b(d_p) d(d_p)\right]\right\}^{-1}, \tag{9a}$$

For $H_{\mathrm{mf}} \le h \le [H_{\mathrm{mf}} + 2(H - H_{\mathrm{mf}})]$.

The flow rate of solids of all sizes removed from the bed

The flow rate of solids of all sizes removed from the bed by the gas flow is calculated by Geldart [21]:

$$F_2 = S\int_{d_{pmin}}^{d_{\mathrm{pmax}}} K^{\bullet}(d_p)\, P_b(d_p)\, d(d_p), \tag{10}$$

where the elutriation constant is calculated as following:

$$K^{\bullet}(d_p) = 23.7\rho_g U_g \exp\left(\frac{-5.4 U_t(d_p)}{U_g}\right) \tag{10a}$$

$$K(d_p) = K^{\bullet}(d_p)\frac{S}{W} \tag{10b}$$

Kunii and Levenspiel [11] correlation is used to calculate the weight of solids in the bed:

$$W = SH(1 - \varepsilon)\rho_{\mathrm{cat}} \tag{10c}$$

The ethylene polymerization rate

The ethylene polymerization rate was adopted based on the model used by Choi and Ray [4] and McAuley et al. [5]:

$$r_{\mathrm{pi}} = K_p C_{ei} \chi_{cat} \rho_p V_{ei}(1 - \varepsilon_i) M_e \tag{11}$$

$$R_{pi} = r_{\,pi}\int_{d_{\mathrm{pmin}}}^{d_{\mathrm{pmax}}} P_b(dp)\, d(dp) \tag{11a}$$

$$K_p = k_{\mathrm{po}} \exp - \left(\frac{E_a}{RT}\right). \tag{11b}$$

Material balance around the Nth compartment

Tanaka [22] has given a correlation for the material balance around the *n*th compartment:

$$k' = \frac{K_{be}\left(U_b - \frac{U_{mf}}{\varepsilon_{mf}}\right)}{\left(U_b + \frac{2U_{mf}}{\varepsilon_{mf}}\right)} \tag{12}$$

$$SU_g C_{b,i-1} = \left(k' V_{bi}\left(C_{b,i} - C_{e,i}\right)\right) + SU_g C_{b,i} \tag{12a}$$

$$K' V_{bi}\left(C_{b,i} - C_{e,i}\right) = R_{pi} V_{ei} \tag{12b}$$

McAuley et al. [5] have given a correlation to calculate the volume of the compartment phases:

$$V_{bi} = S\Delta h_i \delta_i \tag{12c}$$

$$V_{ei} = S\Delta h_i (1 - \delta_i) \tag{12d}$$

The population balance

The population balance is based on a mass balance for particles of size between d_p and $d_p + d(d_p)$, as presented by Kunii and Levenspiel [11,20].

$$F_1 + F_2 + F_o - \sum_{i=1}^{n} R_{pi} = 0 \tag{13}$$

Yong et al. [23] have given a correlation for rate of the increase in particle diameter:

$$(dp) = d\left(\frac{dp}{dt}\right) = \frac{d_{po}\rho_{cat}R_p}{3(1-\varepsilon)d_p^2\rho_p} \tag{13a}$$

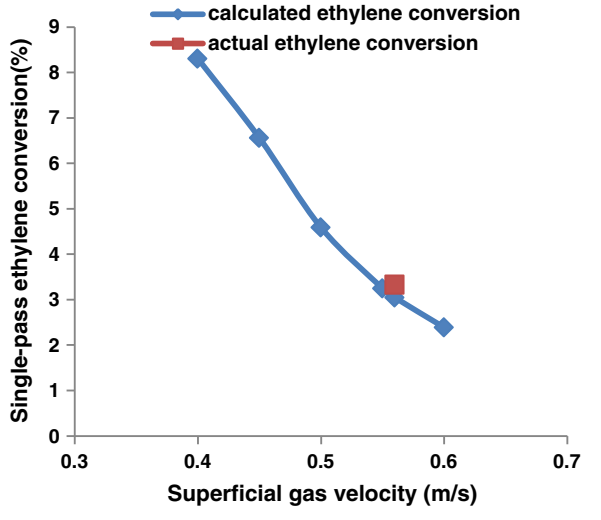

Figure 2 Effect of superficial gas velocity on single-pass ethylene conversion.

The overall mass balance is calculated as:

$$F_o P(d_p) - F_1 P_b(d_p) - WK(r)P_b(d_p) - W\frac{d(dp)P_b(d_p)}{d(dp)} + \frac{3W(dp)\left(P_b(d_p)\right)}{(d_p)} = 0 \tag{13b}$$

Conversion of ethylene

Kunii and Levenspiel [11] correlation is used to calculate the conversion of ethylene:

$$X_A = \frac{22.4\sum R_p T * 1000}{U_g * 3600 * \left(\frac{\gamma C2}{100}\right) * (1.013 * P) * S * 273 * 28} \tag{14a}$$

$$X_A = \frac{C_{Ain} - C_{Aout}}{C_{Ain}} \tag{14b}$$

Results and discussion

Validation analysis

The validation was carried out using the process reported in BP Chemicals [24].The data used in the validation from SidiKerir Petrochemicals Company for the product HD 5502 GA (Alexandria, Egypt) [25] are shown in Table 1. The results of the validation simulations are shown in the data analysis.

Data analysis

The various states of the effect of different variables on the ethylene single-pass conversion have been studied for the following characteristics:

The effects of superficial gas velocity

Industrial fluidized bed polyethylene reactors are operated at superficial gas velocities ranging from three to six times the minimum fluidization velocity [26]. The major effect of an increase in the superficial velocity, U_g, is a reduction in the time required for a given quantity of gas to pass through the bed.

Figure 2 shows the effect of the superficial gas velocity on the percent ethylene conversion. It shows that high gas velocities reduce the conversion of monomer per pass through the reactor and can lead to a greater elutriation of small particles from the bed. Also, the actual ethylene conversion is in the same trend with the chart. Elutriated particles are prevented from passing out from the reactor and into the gas recycle system using a velocity reduction zone at the top of the reactor, where entrained particles are given the opportunity to drop

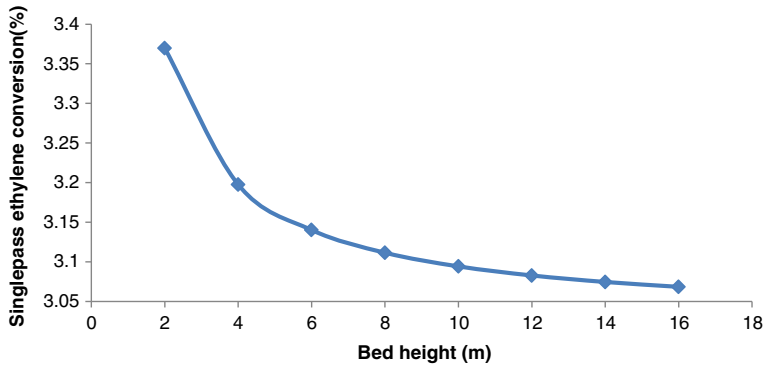

Figure 3 Effect of bed height on ethylene single-pass conversion.

back into the bed. Particle return may also be aided by a cyclone [26].

The effect of bed height

The simulation shows that there is a highly active reaction zone in the top of the reactor; the ethylene conversion decreases by increasing the bed height. It is clear from Figure 3 that single-pass ethylene conversion decreased with increasing bed height. This trend is similar to that found by Fernando and Lona [2].

According to the parametric study of the system, this situation can be avoided by controlling the gas feed velocity. In terms of polyethylene production, it can be enhanced by decreasing the gas feed velocity.

The effect of feed catalyst properties

Figure 4 shows the effect of the catalyst feed rate on the ethylene conversion. It indicates that as the catalyst feed rate increases, the ethylene conversion and particle distribution increase and lead to higher polymerization rates [23].

Figure 5 shows that as Ug decreases from $6U_{mf}$ to $3U_{mf}$, the safe regime, in which the reactor can be operated without a danger of particle melting, decreases accordingly. High gas velocities are required to reduce the risk of particle melting, agglomeration, and subsequent reactor shutdown. However, high gas velocities reduce the conversion of monomer per pass through the reactor and can lead to greater elutriation of small particles from the bed. Elutriated particles are prevented from passing out from the reactor and into the gas recycle system using a velocity reduction zone at the top of the reactor where entrained particles are given the opportunity to drop back into the bed. Particle return may also be aided by a cyclone [26].

Figure 6 shows the effects of catalyst feed rate and bubble size on the single-pass conversion of ethylene. As expected, higher catalyst feed rates lead to higher polymerization rates and to higher conversion. The effects of bubble size on conversion are less obvious. Smaller bubbles have a lower velocity through the bed compared with larger bubbles. As a result, smaller bubbles lead to a larger bubble fraction, δ, in the bed

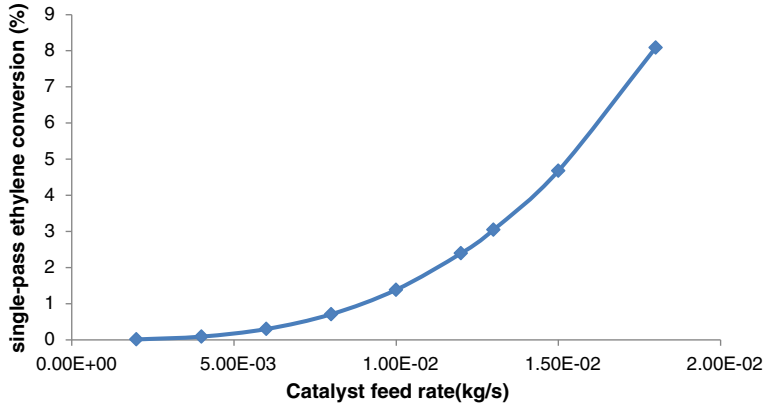

Figure 4 Effect of initial catalyst size on the particle size distribution in the bed.

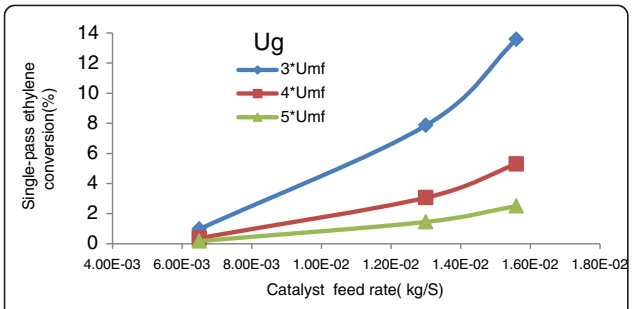

Figure 5 Effect of superficial gas velocity (3 U_{mf} to 6 U_{mf}) and catalyst feed rate on single-pass ethylene conversion.

and to a reduction in the volume of the emulsion phase for a given expanded bed height. Therefore, the residence time for both the solid phase and the catalyst decreases with decreasing bubble size, reducing the quantity of catalyst in the reactor for a given catalyst feed rate. This reduction in the quantity of catalyst tends to reduce R_p, the rate of polymerization, thereby reducing the rate of heat generation in the emulsion phase.

Ethylene conversion

Figure 7 shows a comparison between the calculated conversion and the actual conversion. Good agreement has been observed between the model predictions and the actual plant data. It has been shown that about 0.28% difference between the calculated and actual conversion has been achieved.

Operating variables for sensitivity analysis

Figure 8 shows the sensitivity analysis of the mathematical model using multiplication factors of (0.5, 1, and 1.5) for the variables affected the model. Regarding to catalyst particle diameter, decreasing its value will increase tremendously the single-pass ethylene conversion (by about 4,000 fold); on the other hand, increasing catalyst particle diameter at 50% will decrease the single-pass ethylene conversion to about 0.5% of its original value. Regarding the superficial gas velocity on increasing this value, the single-pass ethylene conversion will decrease. This is understandable since the contact time decreases. From the result shown, it is clear that the single-pass ethylene conversion is not sensitive to change in superficial gas velocity but highly sensitive to catalyst particle diameter. Also, regarding the effect of the total number of compartment, it is clear that increasing total number of compartment in the bed leads to the increase of single pass ethylene conversion. This can be attributed to the increase in the number of compartment in the bed which results in better segregation of the polymer product. It is in accordance with the study results of McAuley et al. [5]. On the other hand, increasing the bed voidage increases the single-pass ethylene conversion. This can be attributed to the increase in bed voidage which would increase the contact surface.

Experimental

The model was solved using Microsoft Excel. The model equations were for the operating conditions shown in Table 1, and the fluidized bed reactor was divided into ten compartments. Each compartment consists of two phases: bubble phase and emulsion phase.

Conclusions

The mathematical model based on the two-phase theory of gas phase fluidization has been developed. The results show that high gas velocities reduce the conversion of monomer per pass through the reactor. The single-pass ethylene conversion decreased with increasing bed height. The ethylene conversion increases as the catalyst feed rate and particle distribution increase. The model has been validated and has shown a good agreement

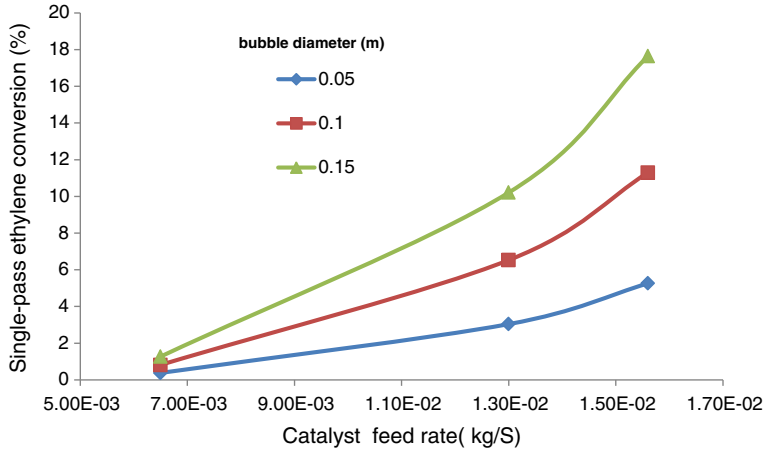

Figure 6 Effect of initial bubble (0.05 to 0.15 m) and catalyst feed rate on single pass ethylene conversion.

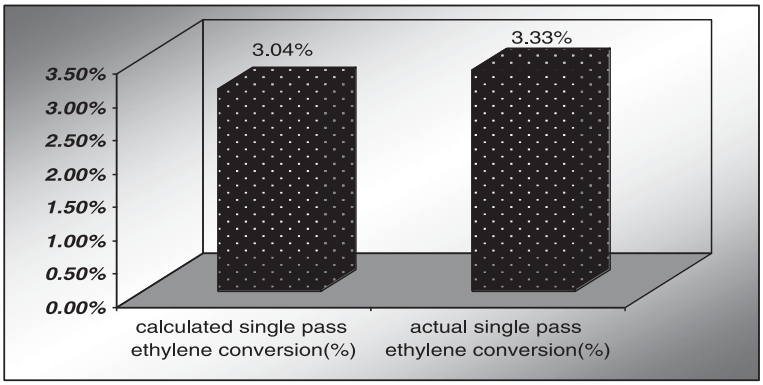

Figure 7 Comparison between actual and calculated ethylene conversions for single pass.

with the actual plant data. The model indicates that the single-pass ethylene conversion is sensitive to catalyst particle diameter, number of compartment, and bed voidage, but change in superficial gas velocity has no significant effect on the model.

Abbreviations

Ar: Archimedes number; C_{Aout}: Ethylene outlet concentration (mol m^{-3}); C_{Ain}: Ethylene inlet concentration (mol m^{-3}); C_{ei}: Monomer concentration in emulsion phase *i*th compartment (mol m^{-3}); d_p: Polymer average particle size(m); d_p^*: Dimensionless particle size; dp_{min}: Minimum particle diameter (m); dp_{max}: Maximum particle diameter (m); d_{po}: Catalyst particle size (m); d_{bo}: Bubble diameter near distributor(m); $d_{b,max}$: Maximum stable bubble diameter(m); $d_{b,i}$: Bubble diameter at (h) height *i*th compartment (m); D_A: Diffusion coefficient for ethylene ($m^2 s^{-2}$); *D*: Reactor diameter (m); E_a: Activation energy (J mol^{-1}); F_o: Catalyst (prepolymer) feed rate (kg s^{-1}); F_1: Flow rate of polymer product (kg s^{-1}); F_2: Flow rate of solids removed by elutriation (kgs^{-1}); *g*: Gravitational acceleration(ms^{-2}); *h*: Bed axial coordinate; *H*: Bed height (m); H_{mf}: Bed height at minimum fluidizing conditions (m); h_n: Distance from the distributor to *n* compartment (m); Δh_1: Initial compartment height (m); Δh_i: Height of *i*th compartment (m); *i*th: Compartment number; K_{bi}: Coefficient of gas interchange in bubble phase *i*th compartment (s^{-1}); K_{ei}: Coefficient of gas interchange in emulsion phase *i*th compartment(s^{-1}); $K_{b,e,i}$: Coefficient of gas interchange between bubble and emulsion phases, overall mass transfer coefficient *i*th compartment (s^{-1}); $K'(r)$: Elutriation constant as a function of *r* (kg m^{-2} s^{-1}); $K(r)$: Elutriation constant (s^{-1}); K_p: Reaction rate constant (m^3 kg_{cat}^{-1} s^{-1}); k_{po}: Pre-exponential factor (m^3 kg_{cat}^{-1} s^{-1}); M_j: Molecular weight of component *j* (kg mol^{-1}); *m*: Proportionality constant relating the bubble diameter; Re_{mf}: Reynolds number at minimum fluidizing condition; N_i: Number of bubbles in *i*th compartment; *n*: Total compartment number; P_b (*d*): particle size distribution in reactor as a function of *r* (m^{-1}); $P_o(r)$: Particle size distribution of feed catalyst (m^{-1}); r_{pi}: Reaction rate in *i*th compartment (kg s^{-1}); *R*: Gas constant (J mol^{-1} K^{-1}); R_{pi}: Reaction rate for whole solid phase *i*th compartment ($kgs-^{1}$); r_{cat}: Catalyst particle radius(m); *r*: Polymer particle radius (m); *S*: Cross-sectional area ($m^2 S = \pi D^2/4$); *T*: Temperature (K); $U_{br,i}$: Velocity *i*th compartment (ms^{-1}); U_t: Terminal velocity of falling particles (m s^{-1}); U_t^*: Dimensionless terminal falling velocity coefficient; $U_t(d_p)$: Terminal velocity of falling particles as function of particle diameter(s^{-1}); U_{bi}: Velocity of bubble rising up through the bed *i*th compartment (m s^{-1}); U_{mf}: Minimum fluidizing velocity (m s^{-1}); U_g: Fluidizing gas velocity (m s^{-1}); V_{bi}: Volume of bubble phase *i*th compartment (m^3); V_{ei}: Volume of emulsion phase *i*th compartment (m^3); *W*: Weight of solids in the bed (kg); X_A: Ethylene conversion; χ_{cat}: Catalyst mass fraction in polymer particle; y_j: Mole fraction of component j.

Greek letters

ρ_p: Polymer density (kg m^{-3}); ρ_g: Gas density (kg m^{-3}); ρ_{cat}: Catalyst density (kg m^{-3}); ρ_j: Density of component j (kg m^{-3}); $R(dp)$: Rate of increase in particle diameter (ms^{-1}); μ_g: Gas viscosity (kg m^{-1} s^{-1}); μ_j: Viscosity of component j (kg m^{-1} s^{-1}); ε_i: Bed voidage of the *i*th compartment; ε: Bed voidage; ε_{mf}: Bed voidage at minimum fluidizing conditions; δi: Bubble fraction for *i*th compartment; Φ_s: Sphericity for sphere particles.

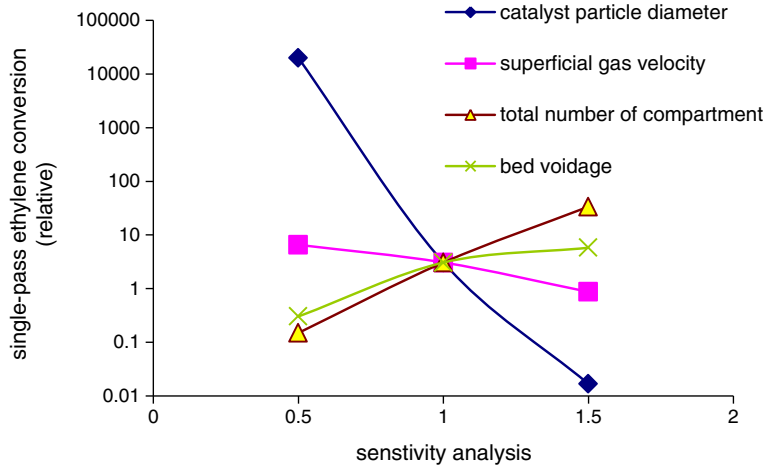

Figure 8 Sensitivity analysis for ethylene conversion.

Competing interest
The authors declare that they have no competing interests.

Authors' contributions
HF and MM drafted the manuscript. MO conceived the study and participated in its design and coordination. YF participated in the design of the study and performed the statistical analysis. All authors read and approved the final manuscript.

Acknowledgment
The authors gratefully acknowledge the faithful support of Eng. Ihab Yahia Abdel-Kader Ahmed (Marketing Research Department Head- SidiKerir Petrochemical Company) for his efforts.

Author details
[1]Chemical Engineering Department, Faculty of Engineering, Alexandria University, Alexandria, Egypt. [2]Petrochemical Engineering Department, Faculty of Engineering, Pharos University, Alexandria, Egypt. [3]City for Scientific Research CSAT, Borg Elarab, Alexandria, Egypt.

Received: 9 November 2012 Accepted: 5 February 2013
Published: 27 February 2013

References

1. University of Michigan (2008) Diffusion and reaction in porous catalysts. http://www.engin.umich.edu/~cre/12chap/html/12prof2a.htm. Accessed 16 January 2012
2. Fernandes F, Lona L (2003) The fluidized bed reactor with a prepolymerization system and its influence on polymer physicochemical characteristic. Braz J Chem Eng 20(2):171
3. Davidson J, Harrison D (1963) Fluidized particles. Cambridge University Press, England
4. Choi KY, Ray WH (1985) The dynamic behaviour of fluidized bed reactors for solid catalyzed gas phase olefin polymerization. Chem Eng Sci 40(12):2261–2279
5. McAuley KB, Talbot JP, Harris TJ (1994) A comparison of two-phase and well-mixed models for fluidized-bed polyethylene reactors. Chem Eng Sci 49(13):2035–2045
6. Hatzantonis H, Goulas A, Kiparissides C (1998) A comprehensive model for the prediction of particle-size distribution in catalyzed olefin polymerization fluidized-bed reactors. Chem Eng Sci 53(18):3251–3267
7. Grosso WE, Chiovetta MG (2005) Modeling a fluidized-bed reactor for the catalytic polymerization of ethylene: particle size distribution effect. Universidad Nacional Del Litoral, Santa Fe, Argentina
8. Kiashemshaki A, Mostoufi N, Sotudeh R (2006) Two-phase modeling of a gas phase polyethylene fluidized bed reactor. Chem Eng Sci 61:399
9. Vahidi O, Shahrokhi M (2008) Control of a fluidized bed polyethylene reactor. Iran J Chem Chem Engn 27(3):87–101
10. Hamzehei M (2011) Study of heat transfer in the poly ethylene fluidized bed reactor numerically and experimentally. WASET 78:522–530
11. Kunii D, Levenspiel O (1991) Fluidization engineering, 2nd edition. Reed Publishing Inc., USA
12. Reid RC, Pransuitz JM, Poling BE (1987) The properties of gases and liquids. McGraw-Hill, New York
13. Wen CY, Fan LT (1975) Models for flow system and chemical reactors. Marcel Dekker, New York
14. Mori S, Wen CY (1975) Estimation of bubble diameter in gaseous fluidized beds. AIChE 21:109–115
15. Cui HP, Moustoufi N, Chaouki J (2000) Characterization of dynamic gas-solid distribution in the fluidized beds. Chem Eng J 79:135–143
16. Kobayashi H, Arai F, Sunagawa T (1967) Chem Eng Japan 31:239
17. Grace JR (1986) Fluid beds as chemical reactors. In: Geldart D (ed) Gas fluidization technology. Wiley, Chichester
18. Haiderand A, Levenspiel O (1989) Drag coefficient and terminal velocity of spherical and nonspherical particles. Powder Technol 58:63–70
19. Specchia V, Baldi G, Sicardi S (1980) Heat transfer in packed bed reactors with one phase flow. Chem Eng Commun 4:361–380
20. Kunii D, Levenspiel O (1969) Fluidization engineering. Wiley, New York
21. Geldart D (1986) Gas fluidization technology. Wiley, Chichester
22. Tanaka T (1967) MSc Thesis. Hokkaido University, Japan
23. Yong KJ, Choi Y, Kyu (2001) Modeling of particle segregation phenomena in a gas phase fluidized bed olefin polymerization reactor. Chem Eng Sci 56:4069–4083
24. BP Chemicals (1996) The Innovene Process- Chromium catalyst technology manual-(Revision 4).:
25. SidiKerir Petrochemicals, Co. (SIDPEC) (2012) DCS PI system. http://www.sidpec.com/PageDetails.aspx?MenuID=3. Accessed 3 January 2013
26. Wagner BE, Goeke GL, Karol FJ (1981) Process for the preparation of high density ethylene polymers in fluid bed reactor. US Patent 4303771:

doi:10.1186/2228-5547-4-20
Cite this article as: Farag *et al.*: **Modeling of fluidized bed reactor for ethylene polymerization: effect of parameters on the single-pass ethylene conversion.** *International Journal of Industrial Chemistry* 2013 **4**:20.